J. Fluid Mech. (1993), *vol.* 256, *pp.* 69–83

Experimental investigation of periodic flow in curved pipes

By CHRIS J. SWANSON†, STEVEN R. STALP AND RUSSELL J. DONNELLY

Department of Physics, University of Oregon, Eugene, OR 97403, USA

(Received 12 November 1992 and in revised form 16 April 1993)

We have studied oscillatory flow through a 180° curved tube with the ratio of tube radius to radius of curvature equal to 1/7. The flow rate is constrained to vary sinusoidally about a non-zero mean at a specified period T, and mean flow rate Q. At a certain parameter range of interest Hamakiotes & Berger (1990) predict that fully developed flow undergoes a period-tripling bifurcation. Our measurements using laser-Doppler velocimetry found no bifurcation. An additional experiment was done to ensure that the flow was fully developed.

1. Introduction

Curved pipe flows have been of considerable interest owing to their application to blood flow in the aorta. Reviews of the subject by Berger, Talbot & Yao (1983), and Ito (1987), summarize recent studies of curved pipe flows and discuss their relation to atherosclerosis. Hamakiotes & Berger (1989, 1990) have found the further interesting phenomenon of period tripling in their numerical solution of the Navier–Stokes equation. The phenomenon of period tripling motivated the present study owing to its possible relation to chaotic flows. Specifically, the numerical simulation predicts that in fully developed oscillatory flow of period T with non-zero mean there is a point in the parameter space at which the T-periodic solution of the equations of motion undergoes a subharmonic bifurcation to a $3T$-periodic solution, that is, period tripling.

Flow is considered fully developed when the velocity field in a cross-sectional slice of the curve is independent of the axial distance downstream from the entrance to the curve (i.e. independent of the angle θ shown in figure 1). In our study we first examined the development of oscillatory flow at many values of θ to determine at what point it becomes fully developed. Then we examined the fully developed region for signs of period tripling.

Oscillatory flow with non-zero mean is characterized by a sinusoidal flow rate of

$$Q = Q_{dc} + Q_{ac}\cos(\omega t + \pi), \tag{1}$$

where $\omega = 2\pi/T$ is the circular frequency of oscillation and T is the period. The flow rate is illustrated graphically in figure 2. A complete description of the flow requires the dimensions of the curved pipe and three dimensionless parameters: the mean Dean number κ_m, the Womersley parameter α (also called the frequency parameter) and the amplitude ratio γ. The mean Dean number is defined by $\kappa_m = 2Re_m\delta^{\frac{1}{2}}$. Here $Re_m = \overline{W_m}a/\nu$ is the Reynolds number of the mean flow with $\overline{W_m}$ being the mean axial

† Present address: Department of Physics, Westmont College, Santa Barbara, CA 93108, USA.

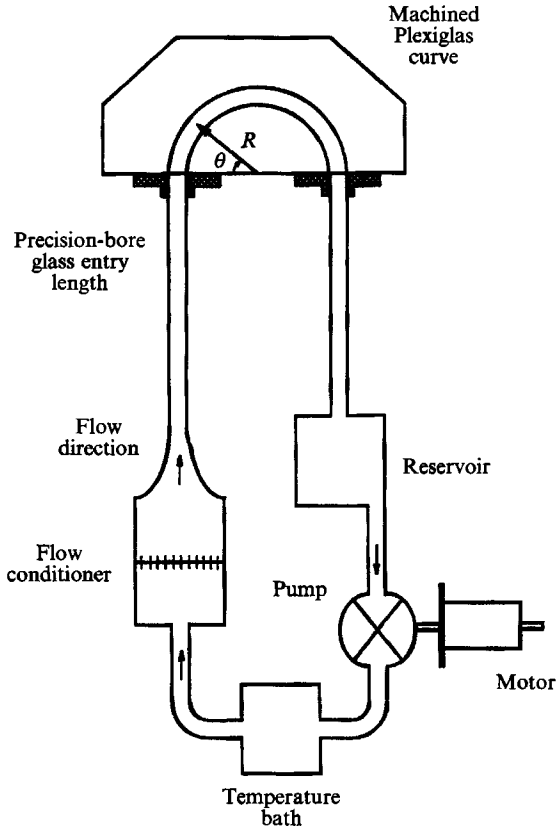

FIGURE 1. Top view schematic of apparatus.

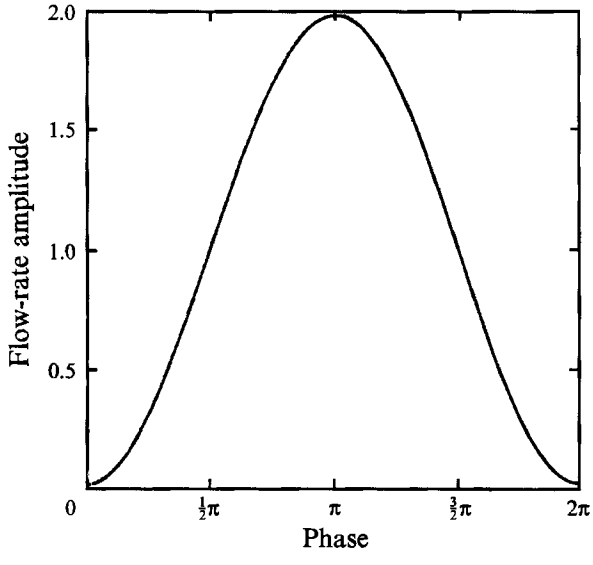

FIGURE 2. Flow-rate amplitude for one cycle of oscillation. The flow rate in dimensionless form is given by $\bar{Q} = 1+\gamma\cos(\omega t+\pi)$, with $\gamma = 0.98$.

velocity, a the radius of the pipe, and ν the kinematic viscosity. $\overline{W_m}$ is related to the flow rate by $Q_{dc} = \pi a^2 \overline{W_m}$. The curved pipe dimensions are described by $\delta = a/R$, which is the ratio of pipe radius to radius of curvature. Since $\delta = 1/7$ through our experiment we chose to use Re_m instead of κ_m. The Womersley parameter is defined by $\alpha = a(\omega/\nu)^{\frac{1}{2}}$. Finally γ is defined as the ratio of AC flow rate to DC flow rate, $\gamma = Q_{ac}/Q_{dc}$. The window of parameter space in which Hamakiotes & Berger found period tripling was for Re_m between 315 and 400, $\alpha = 15$, and $\gamma = 0.98$.

2. Apparatus and error analysis

Our apparatus is shown schematically in figure 1. The curved portion with radius of curvature of 7 cm was machined from a block of Plexiglas providing a very precise geometry. The inlet and outlet tubes were precision-bore glass with 1 cm inner radius. The interface between Plexiglas and glass was made via machined brass connectors, reducing surface discontinuities to approximately 0.3% of the radius. Brass–Plexiglas and Plexiglas–Plexiglas fluid seals were made with rubber O-rings.

Care was also taken to ensure that the inlet flow was as close to fully developed pulsed flow for straight pipes as possible. First the flow was strained by copper wool to reduce large-scale turbulence and it was then funnelled into a straight pipe of 40 diameters length. This inlet condition is to be contrasted with that of Talbot & Gong (1983) who drew fluid from a nearly quiescent reservoir directly into the curve. Although their flow did not become fully developed, the inlet flow condition so affects the subsequent development that we were able to achieve a fully developed state.

Temperature was measured prior to each run and maintained to within 0.1 °C by means of heat-exchanging copper coils submerged in a temperature-regulated bath. A temperature error of 0.1° results in a maximum error in Re_m of 0.2%. Since our fluid was composed of distilled water with only 0.1% impurities (LDV seeding particles), we used an accurate viscosity *vs.* temperature formula taken from Weast (1968, p. F36). The flow rate was calibrated by measuring the flow volume and time directly for various steady-state motor speeds in the exact configuration used for the pulsatile experiment. The relation between motor speed and flow rate was linear and our measurement error was less than 3%. Thus with flow rate, pipe radius, and kinematic viscosity we could calculate the mean Reynolds number with an estimated error of 3%.

The pump was of progressing cavity type which was used to avoid any of the high-frequency pulsations commonly generated by the gears in a more conventional gear pump. Furthermore, the pump was isolated from the experimental platform by means of Tygon tubing to reduce vibrations. The motor was a Compumotor stepping motor, computer controlled to produce a sinusoidal modulation with freedom to change all three parameters from the computer keyboard. We checked the performance of the motor by attaching an encoder having 1000 divisions per revolution on the back shaft of the motor. The measured frequency of modulation agreed to within 0.5% of the computer-selected value. The amplitude of the sine wave was also measured using the encoder and found to agree with the expected value.

The velocity of flow was quantitatively measured by laser-Doppler velocimetry. We used a 15 mW He–Ne laser in backscatter mode to facilitate the orientation and position of the beam crossing. One of the beams was frequency shifted by either 20 kHz or 50 kHz to allow us to filter out the pedestal frequency over the wide range of velocities in each cycle. The laser, frequency shifter, photomultiplier, and focusing optics were mounted and aligned on a small optical bench, and then placed vertically over the curved tube on a sturdy supporting frame (see figure 3). The bench was

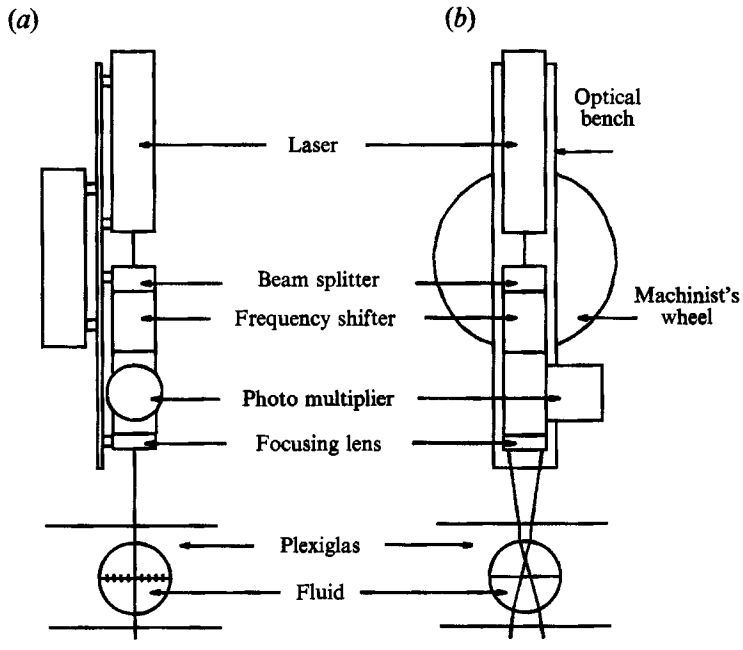

FIGURE 3. Side views of laser-Doppler-velocimetry configurations in backscatter mode. In both views the laser is mounted vertically above the curved pipe. (*a*) Configuration used in measuring the axial velocity profiles. The marks on the horizontal diameter of the curve cross-section denote other points at which the velocity was measured. (*b*) Configuration for measuring velocity perpendicular to the axial flow.

attached to the frame using a machinist's wheel which gave us two degrees of freedom each with resolution of 1/1000th of an inch (one vertical degree of freedom and one horizontal degree parallel to the plane of the beams). However, when measuring the profiles for flow development studies, we needed to adjust the beams orthogonal to the plane of the wheel, and we were only able to make use of the vertical precision. Thus we set a template on top of the Plexiglas block by which we were able to orient the beams manually. The template was removed before taking the data.

The positioning errors were calculated as follows. The centring of the template over the curve was accurate to 0.05 cm. The marks on the template were separated by 0.2 cm and the positioning resolution was approximately 0.05 cm due to the width of the beams. Some calculation was then required to determine the exact position of the beam crossing in the curve since the light was refracted at both air–Plexiglas and Plexiglas–water interfaces. The indices of refraction of these materials are 1.49 and 1.33 respectively with an error of 2%. Thus for the profiles we estimate a maximum positioning error of 0.1 cm or 10% of the radius.

The flow was seeded by 0.5 μm polystyrene beads with a density of 1.05 g/cm^3. Since the density was close to that of water, bead settling was not a problem and we were able to use the same working fluid for over a week. Furthermore, the beads gave sufficient backscattered light for almost every application.

The signal was processed with a TSI IFA550 counter-type processor which includes adjustable low- and high-pass filters as well as an automatic noise rejection feature. To obtain frequency information about the flow it was necessary to take a time series of velocity data. The instantaneous velocity was polled at a well-defined rate using the time base of the PC's internal clock. The average data rate at which the processor

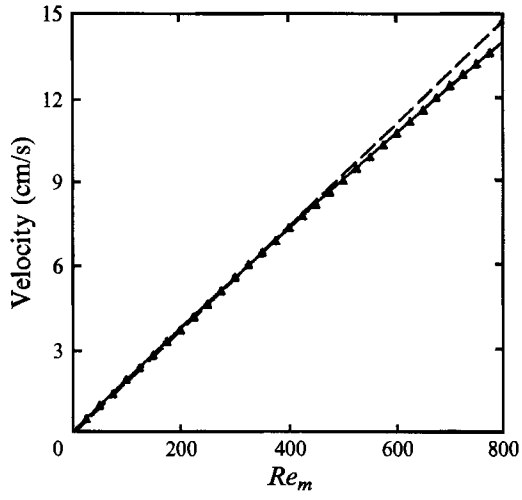

FIGURE 4. Comparison of peak velocity measured with LDV (dashed line) to that of twice the average velocity $\overline{W_m}$ (solid line). The average velocity is derived from the flow-rate calibration of the equation $Q_{dc} = \pi a^2 \overline{W_m}$. The curvature of the solid line arises from the deviation of the profile from a pure parabola.

gathered data varied from 50 to 500 Hz depending on density of seed particles, purity of the water, and depth of the beam crossing. The data rate at which the computer polled the processor was typically of the order of 1–5 Hz, significantly slower than the processor's data rate. In the event of low data rates, the data acquisition program automatically rejected the data. Random noise resulting from time-based errors was at least 40 dB below the power of the primary forced frequency in the fast Fourier transform which suggests that our criteria for acceptable data was sufficient. Since the data could not be sampled from an analog source, analog filtering was unusable and some aliasing of 60 Hz noise was introduced. However, the aliased frequencies were easily identifiable in the FFT power spectrum, creating no problems of interpretation.

In order to estimate the errors in the LDV measurements of velocity, tests were performed on steady flow in a straight pipe. We chose a point in the straight glass tube about 5 cm upstream from the entry to the curve. Here the velocity profile was measured at a Reynolds number of 300 and the peak velocity was measured for Reynolds numbers between 25 and 800. The profile shape at 300 was very nearly parabolic although the best fit through the data did not have zero velocity at the walls. Probably there was some remnant of a boundary layer at this Re_m. We estimate however that the mean deviation of the profile velocities from those of a parabolic profile was less than 5% of the mean velocity. Consequently, the peak velocity should be nearly twice the average velocity as measured by flow rate experiments. A plot of velocity *vs.* Reynolds number is shown in figure 4. The dotted line represents twice the mean velocity from the flow rate calibration $\overline{W_m}$ while the solid line is a best fit quadratic of the velocity in the centre of the tube measured with LDV. It can be seen that the LDV measurements agree to within 2% of the calibrated values for low Reynolds numbers while there is a growing discrepancy at higher Re_m. This discrepancy is a real effect and not an error of measurement since the profile should deviate from parabolic as the boundary layer becomes more significant at higher Re_m. As the profile diverges from a parabola, the peak velocity should become less than twice the mean velocity as seen in the graph. Consequently we estimate that our errors are less than

2% in the centre of the tube where many of the time series measurements were made. Near the edges of the pipe, gradient broadening may become a more significant error as suggested by the profile at $Re_m = 300$ where the best-fit parabola had non-zero velocity at the walls. However, since we are primarily interested in qualitative shape of the profiles, these errors do not invalidate the results.

3. Experimental results

3.1. *Fully developed flow*

In order to compare our experiment with the numerical studies our flow must be fully developed. Since we were working with a curve of only 180° and a δ of 1/7 it is not obvious that such a state is achievable. For *steady* flow with a flat entry profile Yao & Berger (1975) predict that for a Reynolds number of 400 the curve may need to extend up to 600° before the flow is fully developed. However, for steady flow with a *parabolic* entry profile, the estimate is reduced to around 165° (Austin, 1971). For our geometry, flow configuration, and entry conditions, no theoretical or experimental prediction is available. Thus we studied the profiles of the flow at various distances downstream from the entrance.

Figure 5(*a–f*) shows these axial velocity profiles, which were measured across the central horizontal diameter. The parameters for these runs were $Re_m = 325$, $\alpha = 15$, and $\gamma = 0.98$. Each part of the figure represents a different phase of the pumped flow cycle. To obtain the data in this fashion we measured the velocity at equal time intervals six times per period for 50 periods. Then all the measurements at the beginning of each cycle were averaged to give us a single data point for figure 5(*a*). Similarly the second measurements of each cycle were averaged for a point for figure 5(*b*), etc. Thus the corresponding points for figures 5(*a–f*) were gathered simultaneously. The error bars on the data points represent the standard deviation of the mean of the 50 readings per point. It does not reflect the errors in positioning or parameter values. These averaged points and errors were then fit with a least-squares polynomial fit of degree 6 to clarify the form of the profile. The x-axis represents the distance from the inner bend in cm. The angle of curvature from the entry at which each profile was measured is labelled along the left of the figure and the normalized velocity is labelled along the right. (Unfortunately, we were unable to measure profiles at angles between 150° and 165° due to interference from the structural support of the laser and optics.) Each tic mark on the right represents one unit of normalized velocity with the normalization factor being $\overline{W_m}$.

In fully developed flow the profile shape should be completely independent of the angle of curvature. One can see that at the earlier angles of curvature this is not the case. There are slow but pronounced changes in the profiles with respect to the angle of curvature at most of the phases, except perhaps at $\frac{5}{6}\pi$ and $\frac{7}{6}\pi$ when the flow is fastest. With this slowness of development it is difficult to tell if the flow near the outlet has reached its final state. However, since there is little change in the profile shapes for the top three curves, it is possible if not probable that the flow is fully developed after 165°.

In order to substantiate this conclusion we have compared our data at 170° with the numerical solution of Hamakiotes & Berger (1990). We used their fully developed data which was calculated at $Re_m = 375$, $\alpha = 15$, and $\gamma = 0.98$. At this point in parameter space they found period tripling, and thus the flow should repeat itself after not one but three full periods of oscillation. Figure 6 shows a comparison of our experimental data to their data in the first period of oscillation. The curves are least-squares polynomial fits of data gathered by interpolation of their plots. Our data were taken

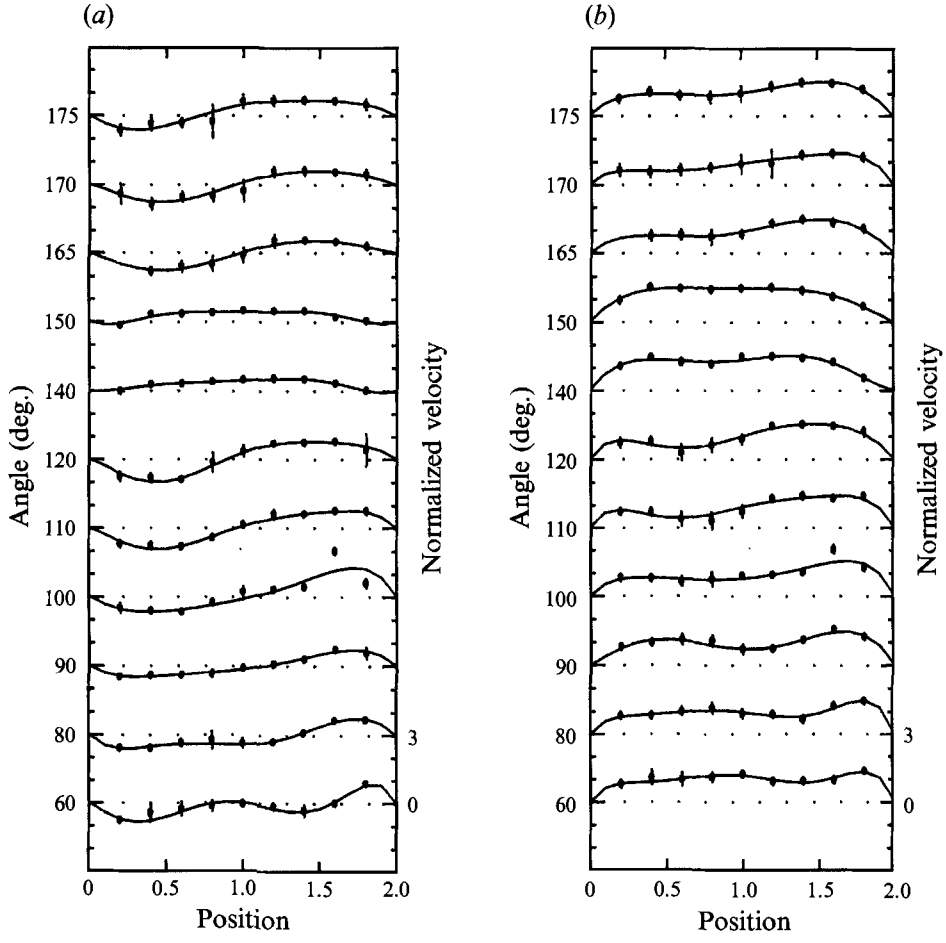

FIGURE 5(*a,b*). For caption see p. 77.

directly from the second profile down (170°) of figures 5(*a–f*) and overlaid on the numerical curves. One can see that there is reasonable agreement at most phases and positions. Figure 7 is identical to figure 6 except that the curves are taken from the second period of the calculations. One can see that the differences in the calculated axial profile from one period to the next are negligible at some phases and positions. At others, there were substantial changes, and many of the discrepancies between our data and their calculations were reduced or eliminated; at still others the agreement became worse in figure 7 than in figure 6. The region of the discrepancy is consistently between 1 and 1.5 cm from the inner bend which is where the greatest changes occur in the calculated profiles from one period to the next. For other regions, where the profiles are independent of period, good agreement between experiment and calculations is found. Thus it seems that the experimental axial flow qualitatively resembles the calculated axial flow but does not give us pertinent information on whether or not the flow is fully developed.

With respect to the secondary flow, we cannot be certain that the axial flow is sensitive enough to show continuing development of the secondary flow. However, in Hamakiotes & Berger's calculations the axial flow was fairly sensitive to the changes in the secondary flow from one period to the next. In fact, the period tripling in the

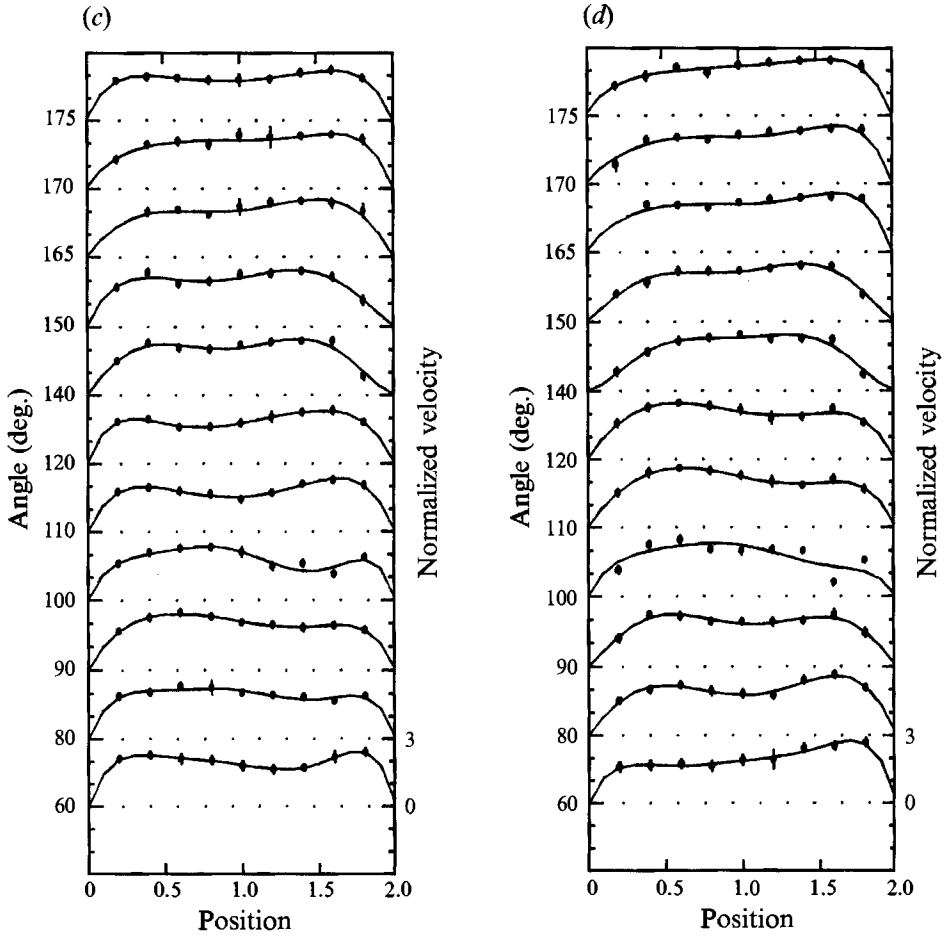

FIGURE 5(*c*,*d*). For caption see facing page.

secondary flow has created the differences mentioned earlier between the curves in figures 6 and 7. Furthermore, while the axial flow as a whole may be relatively insensitive to secondary flow development it seems likely that at least some of the phases and positions in figure 5 should reveal such development. The uniformity of the top three profiles in each part of figure 5 suggests to us that both secondary and axial flow are fully developed. Consequently, we believe that the flow is fully developed within our curve and that the angle at which it becomes so is around 165°.

There remains the possibility that at positions near 180°, beyond which the downstream condition is a straight tube rather than a curved tube, the flow could be modified. Since there is flow reversal near the inner wall of the curved tube, some of the returning fluid may have entered the straight section, and thus the flow at such a position is not the theoretical flow envisioned by Hamakiotes & Berger (1990). We have performed an additional experiment to examine this possibility, described in §4 below.

3.2. *Triply periodic flow*

We utilized a fast Fourier transform algorithm applied to a time series of velocities measured with LDV to search for a subharmonic bifurcation. Although this technique does not give detailed information about the velocity in an entire cross-section, it is far

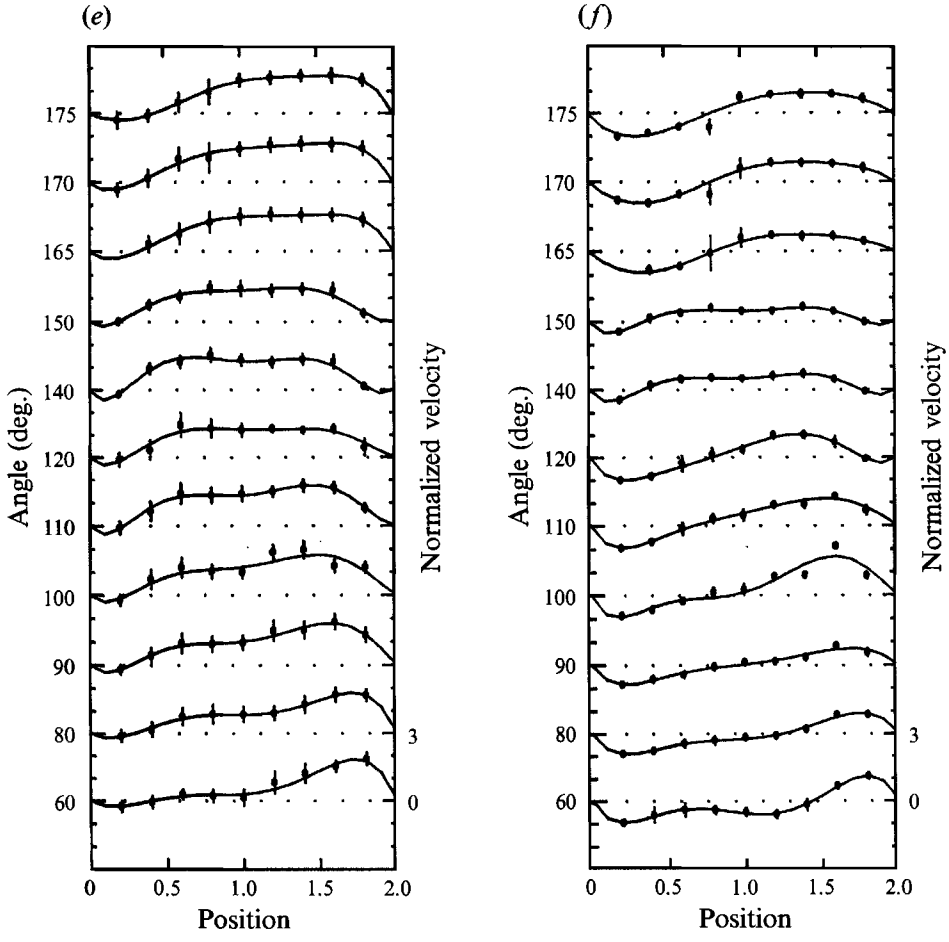

FIGURE 5. Profiles of velocity at various angles of curvature around the bend and at different phases of the flow cycle. Each profile is measured along the horizontal diameter (see figure 3) with the inner bend corresponding to 0 cm. The dimensionless velocity scale $u/\overline{W_m}$ is denoted along the right of each plot. The dotted lines represent the zero velocity base lines for each angle of curvature. (*a*) $\omega t = \frac{1}{6}\pi$, (*b*) $\frac{1}{2}\pi$, (*c*) $\frac{5}{6}\pi$, (*d*) $\frac{7}{6}\pi$, (*e*) $\frac{3}{2}\pi$, (*f*) $\frac{11}{6}\pi$.

less ambiguous and more sensitive when examining frequencies in the flow. Since $3T$-periodicity should exist globally in fully developed flow, we arbitrarily chose a beam crossing point in the centre of the tube, half a radius below the top. The angular distance downstream was 170°. We aligned the plane of the beams perpendicular to the axial flow to examine the circumferential flow. We chose to measure the circumferential flow as it more readily reveals flow pattern details without being overwhelmed by the forcing frequency.

The three parameters Re_m, α, and γ could be controlled from the keyboard, so we were able to make an extensive search of parameter space semi-automatically. A graphical representation of our search is given in figure 8. Note that both the experimental and numerical data presented are for $\gamma = 0.98$. Since the numerical study was limited to this value we also limited our search to a single γ. In figure 8 one can see that the experimental data in open triangles covers the region of proposed period tripling marked with closed squares. We were motivated to implement a dense search along the α-axis because period tripling was found only at $\alpha = 15$ and not at $\alpha = 10$

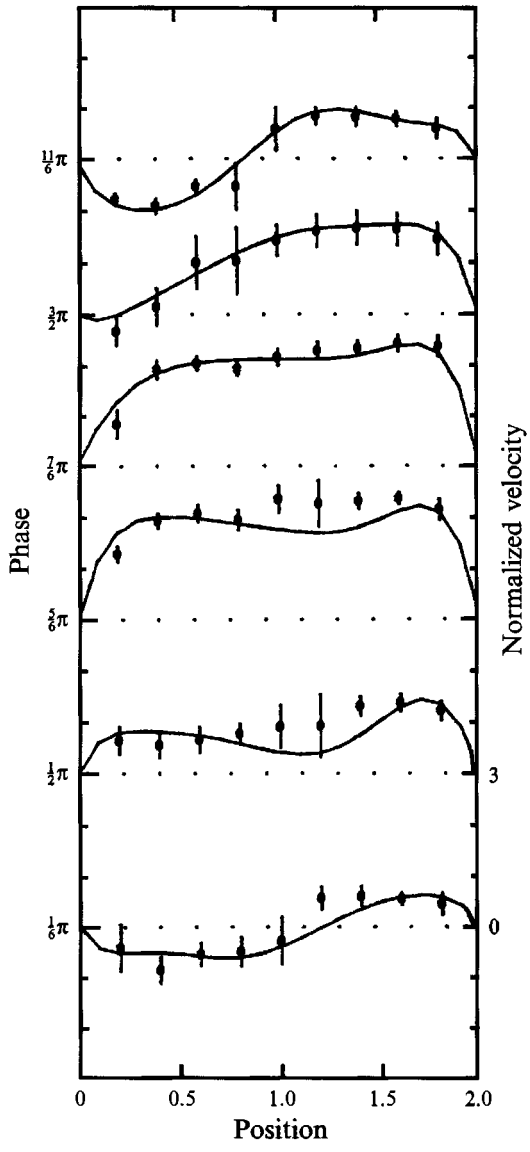

FIGURE 6. Comparison of experimental velocity profile data with numerical curves of Hamakiotes & Berger (1990). The data points are experimental and the curves are numerical. Each profile represents a different phase of the flow cycle at 170° around the curve. The curves were generated from graphical contour plots of the velocity of the first period of oscillation of the period-tripling solution in Hamakiotes & Berger's paper. The contours were interpolated at 9 points along the central diameter and fit with a least-squares polynomial routine.

or $\alpha = 20$. Consequently, it was conceivable that there was a very narrow α-window that we might have missed owing to small errors in our measured value of α. We searched more broadly along the Reynolds-number axis because of the wide range of Reynolds numbers where period tripling was found numerically. Nevertheless, neither the dense search along the α-axis nor the broad search along the Re_m-axis revealed any signs of a $3T$-periodic flow. The distinctive sign of a $3T$-periodic solution that we were looking for was a frequency at one third the forcing frequency in the transformed power spectrum. Since the noise was low we expected that period tripling would show

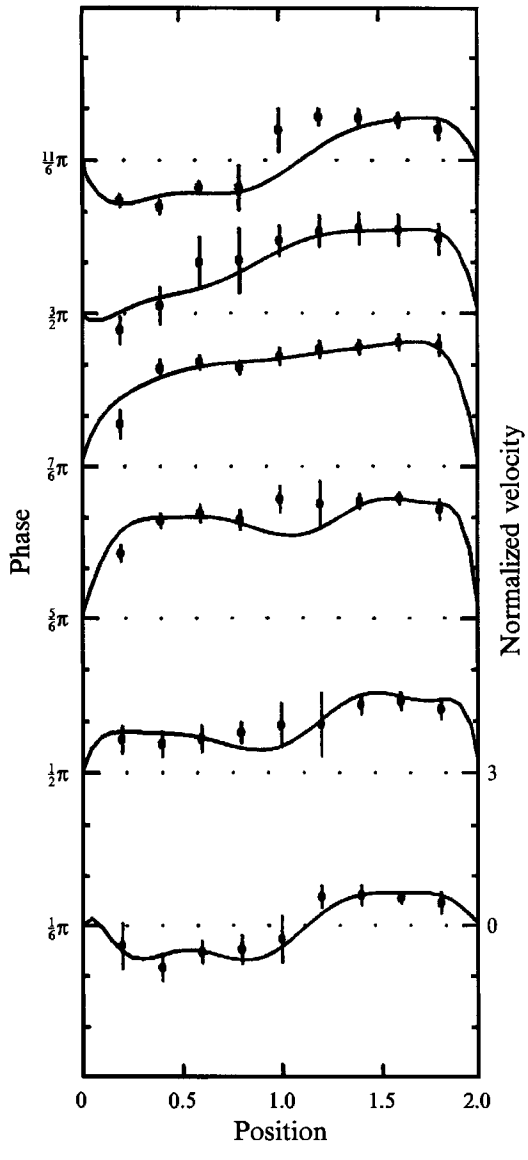

FIGURE 7. As figure 6 except that the curves are from the contour plots of the second period of oscillation of the period-tripling solution.

up as a fairly robust peak, but no statistically significant peaks were ever found at one third. A representative example of the power spectra is shown in figure 9. This spectrum was taken at $Re_m = 350$, $\alpha = 15$, and $\gamma = 0.98$. The primary forcing frequency dominates the spectra at almost 50 dB above the noise floor. The strength of this signal over the noise indicated the sensitivity of the measurement. Smaller peaks equally distributed about the primary frequency are aliases of 60 Hz noise and other combinations of 60 Hz and the forcing frequency. These small peaks were present in most all of the spectra, but were always easily identifiable.

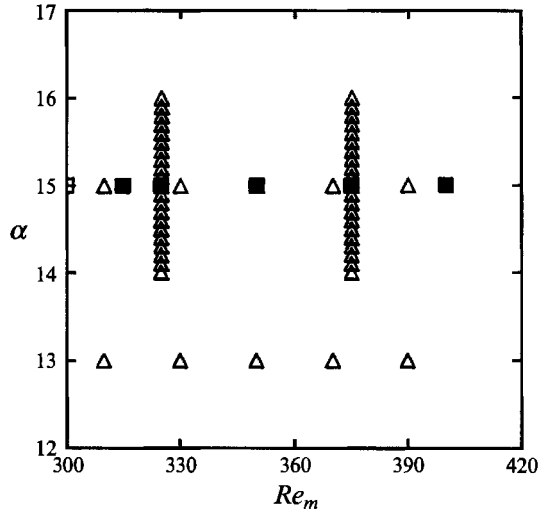

FIGURE 8. Two-dimensional parameter space plot with γ fixed at 0.98. Closed squares represent numerical calculations where period tripling was found. The open square on the left represents numerical calculations without period tripling. Triangles are points of parameter space examined experimentally with the 180° curved pipe.

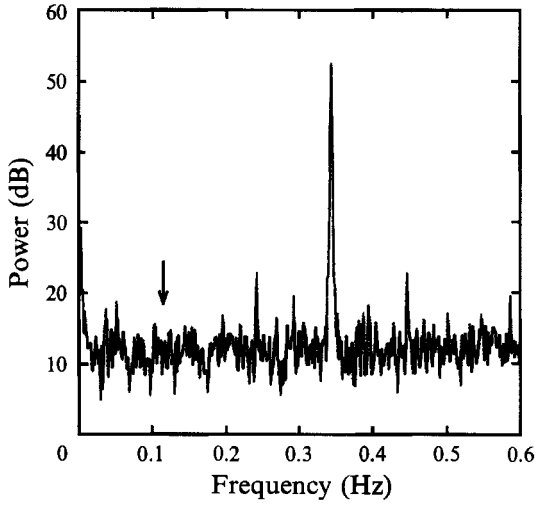

FIGURE 9. A typical power spectrum of a velocity time series. Parameter values for this spectrum were $Re_m = 375$, $\alpha = 15$, and $\gamma = 0.98$. The strong peak signifies the frequency of forcing, $f = 0.344$. The arrow points to a frequency of $\frac{1}{3}f$ where a peak would exist if period tripling were found.

4. Further experiments with a spiral tube

Despite significant efforts to determine if the flow in the 180° curve was fully developed, firm conclusions could not be drawn. Thus a further study of the flow was undertaken. A second apparatus was constructed from Tygon tubing wrapped six times around a central post as shown in figure 10. The dimensions of the tubing closely matched the dimensions of the previous experiment so that the 180° curve could be easily replaced by the wrapped tube system. Consequently the various flow parameters were determined and controlled precisely as before. The tube's inner diameter was

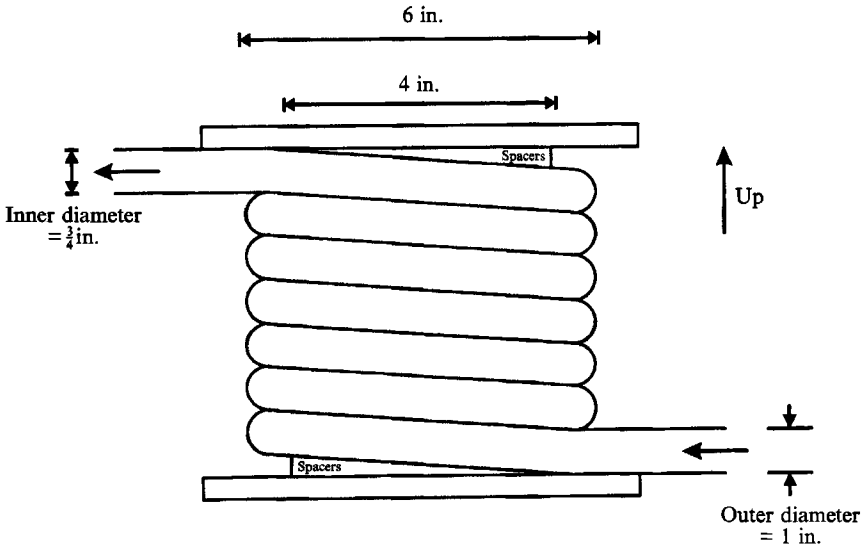

FIGURE 10. Side-view drawing of helical apparatus with fully developed flow.

0.75 in.; the outer diameter was 1.00 in.; and the diameter of post was 4 in. Thus the ratio of tube radius to radius of curvature was kept at 1/7 as required. While wrapping the tubing, care was taken to maintain as close to a circular cross-section as possible. However, some stretching was inevitable. Measurements of the cross-section revealed that the tube took on a slightly elliptical shape with minor and major axes of 1.96 cm and 1.63 cm respectively.

Data were taken at 4π, 6π and 8π radians downstream from the inlet. These intermediate angles allowed the flow sufficient time to become fully developed and at the same time kept the flow adequately buffered from downstream effects. Since the flow was assumed to be fully developed, no velocity profiles were needed and a simpler flow visualization technique could be employed. The flow was seeded with Kalliroscope reflecting platelets which aligned themselves with the shear of the flow (Matisse & Gorman 1984). The reflectance of the fluid was measured at a point by reflecting a 1 mW He–Ne laser beam from the fluid into a photo detector. The measured reflectance was very sensitive to patterns in the flow.

A time series was taken and analysed with an FFT as was done previously. One such time series is shown in figure 11. The strong peaks correspond to the frequency of forcing and its higher harmonics. No peak was found at one-third of the forcing frequency, which would indicate period tripling. It is to be noted that the signal-to-noise ratio of the forcing frequency was 40 dB above the noise, indicating that this flow visualization technique was as sensitive as the LDV. As before, a broad search of the parameter space was carried out which included, but was not restricted to, Re_m from 250–450 in steps of 25, γ from 0.9–1.0 in steps of 0.02, and α from 14.5–15.5 in steps of 0.25. These parameters were searched at 4π, 6π and 8π radians downstream from the inlet yielding a null result in every measurement.

By measuring the secondary velocity vectors at specific points in the figures of Hamakiotes & Berger (1990), we were able to get an order of magnitude estimate of how large the peak in the power spectrum at one third the forcing frequency might be in comparison to the driving frequency peak. The height of the peak in the power spectrum at the forcing frequency is associated with the change in the velocity field

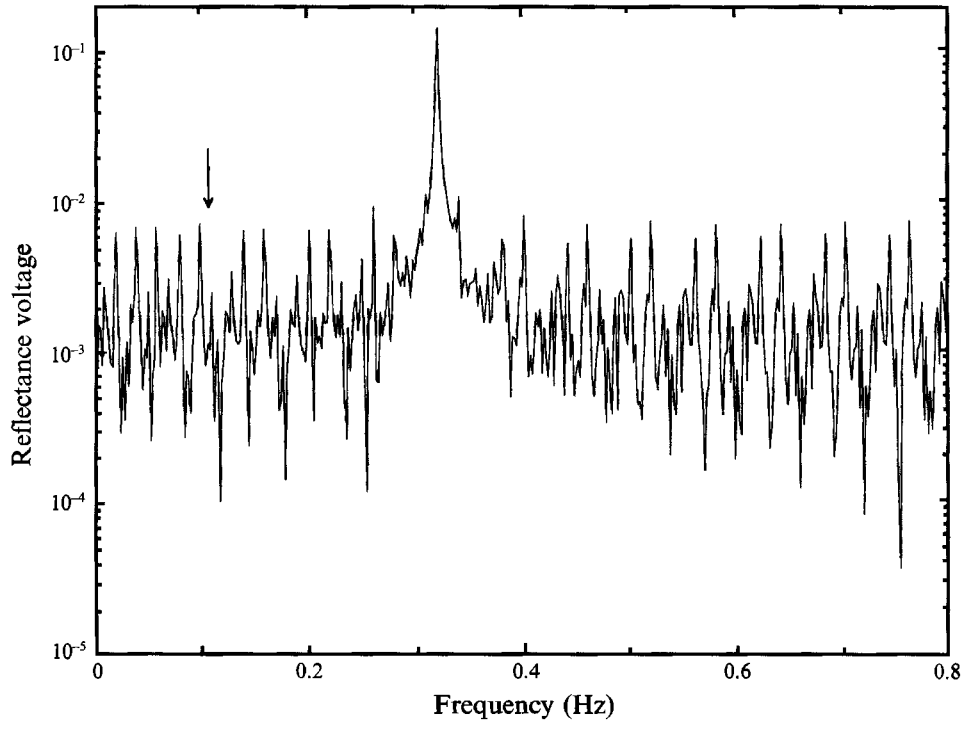

FIGURE 11. Fast Fourier transform of reflectance voltage using 1024 data points. Parameter values for this spectrum were $Re_m = 350$, $\alpha = 15.0$, $\gamma = 0.98$. The strong peak signifies the frequency of forcing, $f = 0.322$.

from phase to phase in the same cycle and the height of the expected peak at one third the forcing frequency is associated with the change in the field at the same phase but at the three different cycles. The difference between these two measurements was of the same order of magnitude, which implies that the height of the peak in the power spectrum where period tripling is expected (see figure 11) would be comparable to the height of the driving frequency peak. Thus the expected peak at one third the forcing frequency is not obscured by the background signal.

We conclude that if period tripling exists it is apparently destroyed by either an elliptical perturbation in the cross-section of the curve or by a small pitch.

5. Conclusions

We have studied the development of the flow in a 180° curved pipe subject to a sinusoidal flow rate, and the frequency characteristics of the flow in the final 15°. Profiles of the axial flow at various angles of curvature around the bend have been measured for different phases of the flow cycle. These profiles indicate that the entry length for fully developed flow may be around 165° for $\delta = 1/7$. Beyond this point the profiles are nearly identical and show little if any development. Furthermore we have compared the profiles in this region of the bend to the numerical work of Hamakiotes & Berger (1990) and found some agreement within specific regions in support of the conclusion of fully developed flow.

However, in the frequency domain we found no evidence for the predicted period tripling. We suggest some possible reasons for this failure. First, it is possible that in

the 180° curve the flow is not fully developed and the axial profiles are insensitive to further development of secondary flow. Yet, our additional experiment certainly achieves full development of the flow and still no period tripling is found. This additional experiment, however, may be criticized for imperfectly matching the geometry used in the computer calculations. Secondly, it is unlikely that the solution of an unsteady calculation would be unstable, especially since the calculated solution was so robust. However, it is possible that the numerical solution using the assumption of fully developed flow could differ from a solution arrived at in a four-dimensional calculation of developing flow. This type of convectively unstable solution could be examined by further numerical study. Thirdly, for multiple parameter systems, stability theory states that only an extremely narrow window of parameter space exists in which a period-three solution would be expected. It is possible that the window in γ-space or α-space is so narrow that our search did not uncover it. Since a similarly narrow window should exist for the numerical solution, this hypothesis could be tested if further calculations explored values of α and γ very close to 15 and 0.98. Finally, it is possible that the period-tripling state is not unique, and one must vary the parameters according to a specific protocol to obtain the desired state. However, considering the robustness of the numerical solution to various choices of temporal and spatial discretization, we feel this to be unlikely. Note that the large dimensionality of parameter space makes an uninformed experimental search for a proper protocol impractical.

We are much indebted to Stanley Berger for his constant encouragement in making these measurements and for many useful discussions. We are grateful to the late Don Nickles for his assistance in design and construction of the apparatus. This work was completed with the support of the National Science Foundation Condensed Matter Physics Program under Grant DMR-91-18924.

REFERENCES

AUSTIN, L. 1971 The development of viscous flow within helical coils. PhD thesis, University of Utah.

BERGER, S. A., TALBOT, L. & YAO, L. S. 1983 Flow in curved pipes. *Ann. Rev. Fluid Mech.* **15**, 461.

HAMAKIOTES, C. C. & BERGER, S. A. 1989 Period tripling in periodic flows through curved pipes. *Phys. Rev. Lett* **62**, 1270.

HAMAKIOTES, C. C. & BERGER, S. A. 1990 Periodic flows through curved tubes: the effect of the frequency parameter. *J. Fluid Mech.* **210**, 353.

ITO, H. 1987 Flow in curved pipes. *JSME Intl. J.* **30**, 543.

MATISSE, P. & GORMAN, M. 1984 Neutrally buoyant anisotropic particles for flow visualization. *Phys. Fluids* **27**, 759.

TALBOT, L. & GONG, K. O. 1983 Pulsatile entrance flow in a curved pipe. *J. Fluid Mech.* **127**, 1.

WEAST, R. C. 1968 *Handbook of Chemistry and Physics*, 52nd Edn. Chemical Rubber Company.

YAO, L. S. & BERGER, S. A. 1975 Entry flow in a curved pipe. *J. Fluid Mech.* **67**, 177.